2.

Presented at the International Conference on Lasers
Lake Tahoe, Nevada - December 6-9, 1993

CONF-931237--8

BNL-60088

10-GW CO_2 LASER SYSTEM AT THE BROOKHAVEN ACCELERATOR TEST FACILITY*

I. Pogorelsky, J. Fischer, A.S. Fisher, T. Srinivasan-Rao
Brookhaven National Laboratory
Upton, NY 11973

N.A. Kurnit, I. J. Bigio, R. F. Harrison, and T. Shimada
Los Alamos National Laboratory
Los Alamos, NM 87545

K. Kusche, M. Babzien
SUNY at Stony Brook
Stony Brook, NY 11794

Abstract

Design and performance of a high peak-power CO_2 laser system to produce subnanosecond IR pulses for electron acceleration experiment are presented. We discuss theoretical aspects of the picosecond laser pulse propagation in a molecular amplifier and a design approach towards compact Terawatt CO_2 laser systems.

I. Introduction

High-power gas laser development for strong-field physics and other applications has been an active area of quantum electronics since the advent of lasers. Gas lasers are attractive for building economical high-aperture, large-volume modules with high energy output. But because of the relatively narrow rotational structure typical for molecular gas spectra ($\approx 10^{10}$ Hz), the generation and amplification of ultra-short pulses in CO_2 lasers has not been as successfully pursued as in the case of solid state lasers having a wide crystal-host broadening of the individual ion spectral lines ($10^{11} - 10^{12}$ Hz).

Over the years, substantial progress has been made on ways to produce high-power pulses on a sub-nanosecond time scale from CO_2 lasers. Apart from self-mode-locking, the list of CO_2 picosecond pulse generation methods includes: optical free-induction decay (OFID),[1] optical parametric oscillator,[2] and semiconductor switching.[3,4] The OFID method is based on the CO_2 pulse self-quenching in a plasma shutter followed by its futher shortening in a hot CO_2 absorption cell. Using this method, 30-300 ps variable duration CO_2 pulses were produced. The other two methods are active; the first uses a short-wavelength picosecond source for generating by parametric pumping the radiation to be amplified, the second uses a picosecond source to create free carriers in a semiconductor that acts as a shorted-lived reflecting plasma for CO_2 radiation. This method can produce CO_2 pulses down to the width of the control pulse and even shorter. By semiconductor switching and consecutive regenerative amplification, up to 1.5 GW 3-ps CO_2 laser pulses were demonstrated.[5]

The semiconducting switch pulse generation method is used in a multi-GW CO_2 laser system comprised of a hybrid TEA single-longitudinal mode CO_2 oscillator, and a UV-preionised 3-atm multipass TE CO_2 amplifier. This system is now operational at the Brookhaven Accelerator Test Facility[6] (ATF) to test several laser acceleration and FEL schemes in which a high-power CO_2 laser beam interacts with a 50 MeV e-beam produced by an RF linac.

*This work was performed under the auspices of the U.S. Dept. of Energy.

II. Picosecond pulse slicing

The picosecond switching method used in the ATF CO_2 laser system is based on modulating the reflective and transmissive properties of a semiconductor by optically controlling the free-carrier charge density. A short-wavelength picosecond laser pulse with a photon energy above the band gap of the semiconductor creates a highly reflective electron-hole plasma in a surface layer of a semiconductor, such as germanium, which is normally transparent to 10-μm radiation. The free-electron density at the semiconductor surface is linearly proportional to the absorbed control-pulse fluence. At a Nd:YAG control pulse fluence of $E \approx 2$ mJ/cm^2, the density of excess free carriers created in Ge is more than 2×10^{19}/cm^3, which is just above the critical electron density $N_{cr} = 1.6 \times 10^{19}/cm^3$, and a Ge slab switches from a window at 10 μm to a highly reflective mirror.

After the termination of the control pulse, the main process governing the time evolution of the excess free carriers at the surface, and hence the reflectivity, will be ambipolar diffusion:[3] having a characteristic time constant of 150 ps in Ge. To define the trailing edge of the pulse, shortening it to a few picoseconds, the complement to reflection switching, transmission switching, is used for a second stage. An optically delayed control pulse cuts off the trailing edge of the transient pulse by initiating reflection and absorption. Absorption makes the Ge slab opaque for 10-μmradiation during $\approx$50 ns time while the electron-hole recombination takes place. The resulting "sliced" transmitted pulse has the desired few- picosecond length determined by optical delay adjustment of the control radiation before the transmission switch.

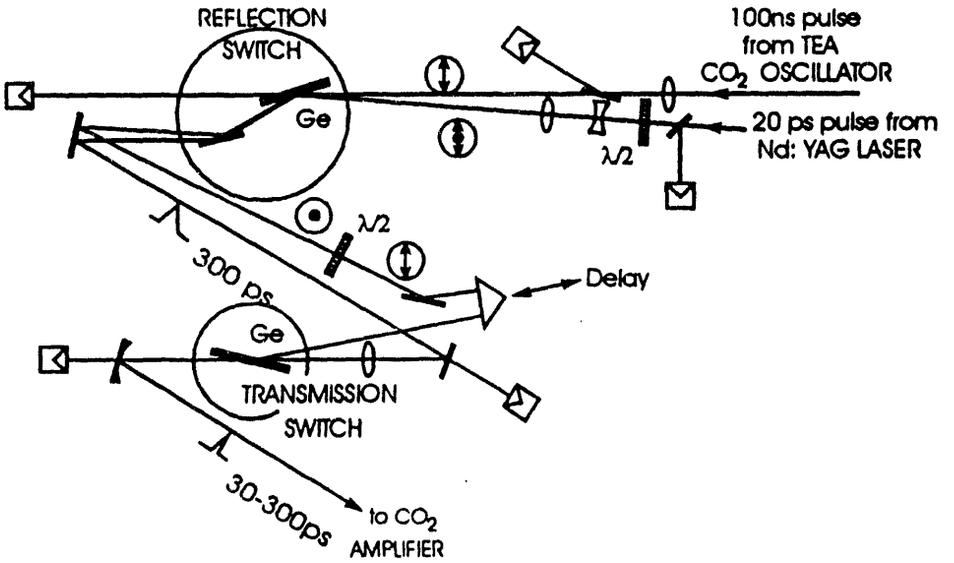

Figure 1: Principle diagram of the CO_2 pulse semiconductor 2-step slicing.

The schematic of the optical set up used in the experiment is presented in Fig.1. The hybrid single-longitudinal sero-transverse mode TEA CO_2 laser oscillator is the source of the 10 μm beam. Single-longitudinal-mode operation is provided by a combination of a low-pressure auxiliary discharge tube used to provide a narrow peak in the gain spectrum and pieso-electric fine tuning of the oscillator cavity length. A polarisation rotation of the control Nd:YAG beam provides optimal distribution of the control pulse energy between the reflection and transmission switches. CO_2 laser peak power after slicing is $\approx$0.5 MW with a contrast ratio of 10,000:1.

III. Multipass amplifier

A 3-atm multipass CO_2 amplifier pumped by a UV-preionized transverse electric discharge serves to increase the peak power of the sliced picosecond 10-μm pulse from 0.5 MW up to the $\approx$10-GW level required for the electron acceleration experiment. The laser amplifier head consists of a cylindrical plexiglas vessel designed to house the main discharge electrodes and the preionizing spark-gap arrays. Two sets of serially-placed brass electrodes define the discharge volume of 2x5x60 cm^3 (x2) = 1,200 cm^3. Preionization spark-gap arrays are arranged in series along the side walls of the discharge volume and a sliding spark is excited by a 35 kV voltage pulse. The amplifier cell rests on an oil tank containing the high-voltage pulse-forming circuit. Two sets of 2-stage Marx generators supply up to 140 kV pulses to the main discharge with a specific energy loading of up to 650 J/l. Triggering of the preionization and the two main discharge sections is accomplished through five pressurized-air spark gaps.

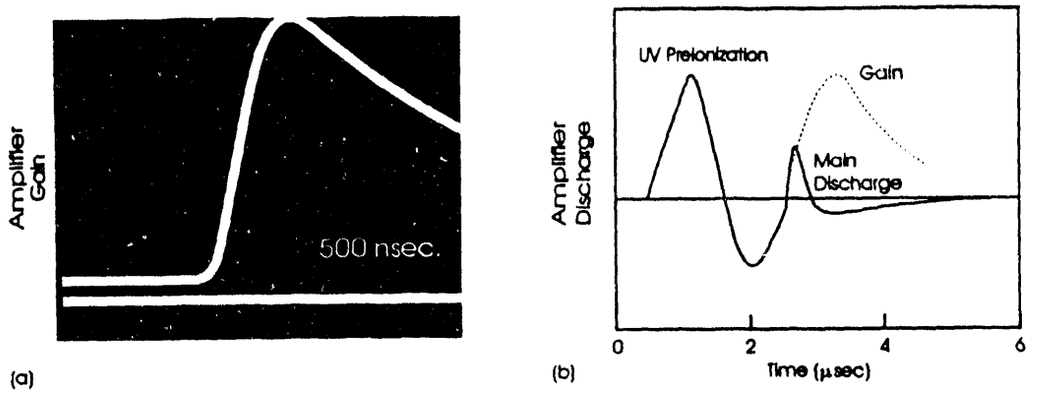

Figure 2: Amplifier temporal characteristics: a) small signal gain trace probed with a CW CO_2 laser; b) preionization and main discharge electrical signals with a gain (dashed curve) superimposed.

Requirements of arc-free and mechanically safe operation of the amplifier discharge cell place a 3-4 atm limit on the working gas pressure. Gas mixture CO_2:N_2:He=1:0.5:8.5 was normally used. Small signal gain (SSG) up to 2.4 %/cm at 10.6 μm was measured under these conditions. The scope trace of the gain probed with a CW CO_2 laser and discharge signal are presented in Fig.2. By adjustment of the timing of the discharge triggering, the multipass propagation of the laser pulse is made to coincide with the maximum gain in the amplifier.

The closed-loop gas supply manifold includes a diaphragm-type compressor with a capacity of 0.8 CFM and a catalytic regenerator. Low rate gas exchange inside the amplifier volume is arranged through two symmetrical axial gas flows directed from the end flanges holding ZnSe Brewster optical windows towards the exhaust port in the central portion of the amplifier cell. Catalytic regeneration of the gas mixture during its closed-loop circulation through the amplifier serves to maintain stable discharge and gain conditions.

Using the configuration shown in Fig.3, as many as 8 optical passes were accommodated through the amplifier cell with a total up to 10^{10} net SSG (for a long pulse). A concave mirror with a 20 m radius of curvature is used after 2 passes to compensate for beam divergence. A roof mirror arrangement at the other side of the amplifier helps to prevent parasitic optical resonances inside the amplifier. Four passes may be arranged in this way without self-lasing. Due to the limited aperture of the amplifier cell, no additional mirrors may be placed without creation of a quasi-stable cavity and self-lasing build-up. Consequently, the same 4-mirror set is used for an additional 8 passes. To suppress parasitic feedback through the optical path while redirecting the beam for the next 4 passes, an optical polarization isolator is placed in the way of the amplified beam.

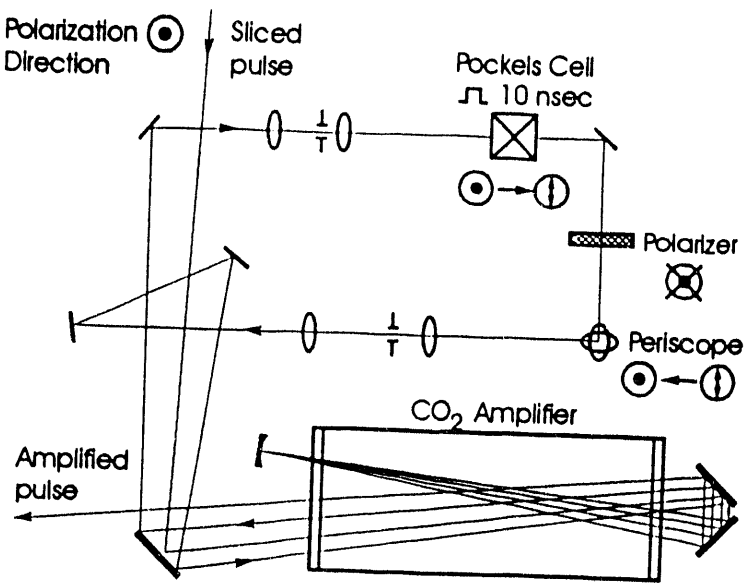

Figure 3: 8-pass amplifier optical set up.

The optical isolator consists of a polariser (germanium Brewster plate) with a Pockels cell in front of it. The polariser is set in a crossed orientation to the ZnSe Brewster windows of the amplifier. By applying a 10-ns 8-kV pulse to the Pockels cell synchronously with the picosecond laser pulse arrival, we turn its polarization 90° and transmit the pulse through the polariser. A 90° rotating periscope is used for polarisation correction after the isolator before sending the transmitted pulse for another 4-pass course of amplification. Telescopes are designed to adjust beam diameter and divergence and to produce an additional discrimination against the self-lasing by using pin-hole diaphragms in focal points.

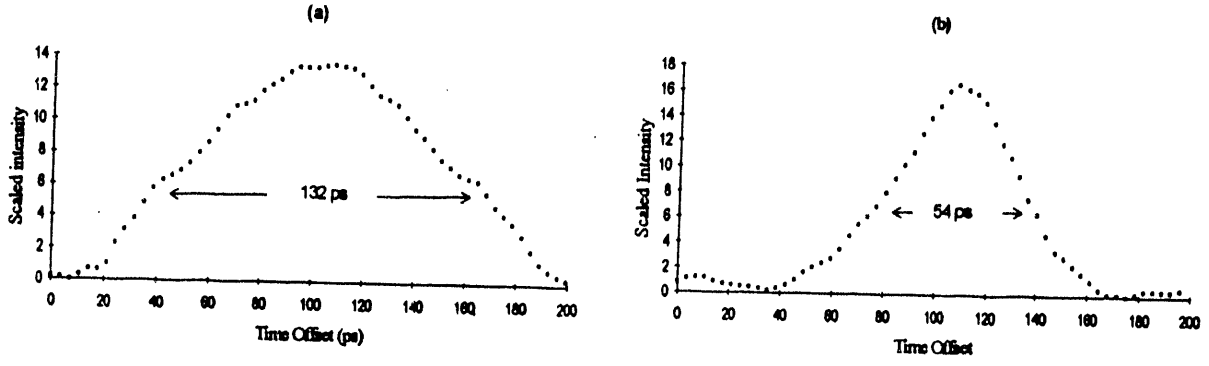

Figure 4: Experimental autocorrelation curves for the amplified single-switched CO_2 laser pulse: a) without a self-breakdown and b) with a self-breakdown.

Another important function of the telescope in front of the Pockels cell is shortening of the amplified pulse through the optical breakdown on a pin-hole diaphragm. A single-shot autocorrelator based on noncollinear second harmonic generation in a $ZnGeP_2$ crystal was used to monitor the amplified CO_2 laser pulse duration.

Sample autocorrelation curves recorded for 6-pass amplified CO_2 pulses, obtained for input transient pulses with and without a self-breakdown after 4 passes, are presented in Fig.4. The duration of the laser pulse after self-breakdown is regulated by the time required for the optical breakdown development and does not depend much upon the initial duration of the sliced pulse. The effect is reproducable from shot to shot. It indicates, that a simple laser plasma shutter is efficient for pulse duration control during subnanosecond pulse amplification.

Fig.5 shows energy evolution when various duration laser pulses are sent for amplification. The similarity of the pulse duration after self quenching, together with a saturation effect, may explain, why all three experimental curves terminate after 8 passes through the amplifier at about the same output energy of $\approx$1 J corresponding to a peak power of 15...25 GW in $\approx$50 ps pulse.

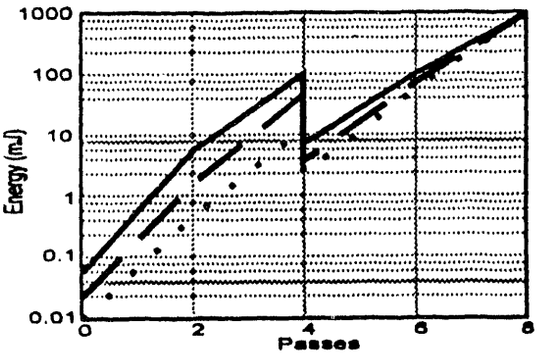

Figure 5: Experimental curves for laser pulse evolution in 8-pass amplifier: (solid line) single-switched initial pulse; (dashed line) 120-ps sliced initial pulse; (dotted line) 60-ps sliced initial pulse.

IV. Picosecond pulse shaping in the CO_2 amplifier

In order to understand, why we are limited to a 50-ps pulse when a 3-atm CO_2 amplifier is used, we should consider specifics of short laser pulse propagation in a resonant-amplifying molecular medium.[7] Two characteristic spectral parameters and their corresponding time constants should be taken into consideration. The first is a time, δt_1, corresponding to a frequency interval, $\delta\nu_1$, between the centers of V-R lines by the ratio $\delta t_1 = \delta\nu_1^{-1}$; δt_1=18 ps for the P-branch of the 10-μm CO_2 band. The other is a collisionally induced dipole dephasing time, δt_2, related to a Lorentzian line shape of a V-R transition by the similar ratio $\delta t_2 = \delta\nu_2^{-1}$; δt_2 is inversely proportional to the gas pressure and $\delta t_2 \approx$100 ps for 1 atm CO_2 laser gas mixture. Let us consider, how the amplification of the CO_2 laser pulse with the initial duration τ_0 depends upon the time constants δt_1 and δt_2.

The spectral width of a short laser pulse (less than δt_1) may cover several discrete transition lines. The electric field of such an input pulse excites a polarization in CO_2 molecules, which are in various V-R states. Since molecules in different states are characterized by different frequencies, these polarization components eventually become dephased. As a result, the spectral and time structure of the induced radiation will not remain equal to those of the initial pulse. At a low gas pressure the discrete gain spectrum transforms the spectrum of the input pulse from continuous to discrete, and its Fourier transform corresponds to a pulse train with a δt_1 period. At higher pressure, the broadening effect smooths the discrete gain spectrum. An alternative to achieve gain smoothing is a reduction of the spectrum modulation period using an isotopic gas mixture. Replacement of one of the oxygen nuclei by that of a different isotope destroys a symmetry of the CO_2 molecule. That means that twice as many V-R transitions are allowed and the gain spectrum becomes twice as dense as with a regular CO_2 molecule. If we consider a mixture $^{13}C^{16}O_2$: $^{12}C^{16}O^{18}O$: $^{12}C^{18}O_2$ = 1:2:1, then, due to isotopic shifts, the combined spectrum will have in overlap regions an approximately 4-times denser rotational line structure than with a regular CO_2 molecule. Computer modeling[8] shows that the reduction in spectral line interval results in considerably less short-pulse distortion during amplification (see Fig.6).

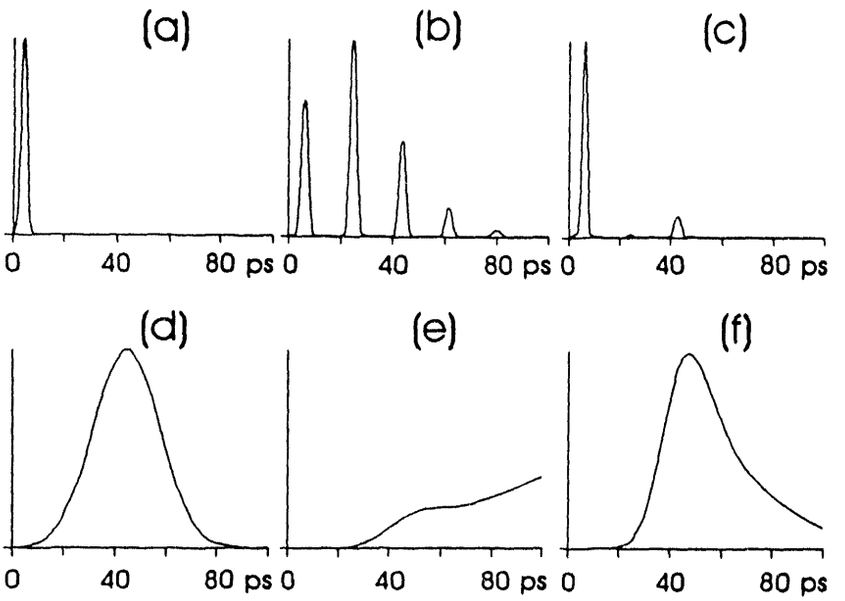

Figure 6: Picosecond pulse propagation in the CO_2 amplifier with a total gain $g_0 l = 10$ (initial intensity 1 MW/cm^2)[8]: a) initial 3-ps pulse shape; b) same after amplification in a regular 10-atm mixture; c) same in a 4-atm isotopic mixture; d) initial 30-ps pulse shape; e) same after amplification in a 1-atm regular mixture; f) same in a 10-atm regular mixture.

If the input laser pulse width, τ_0, is longer than δt_1, then just one rotational line is involved in the amplification. During the amplification, the spectrum of the input pulse is filtered by the gain spectrum and eventually pulse duration increases. Pulse broadening is most pronounced at atmospheric or lower pressure, when the spectral width of the individual V-R transition is much less than the spectral separation between the rotational lines, and the gain spectrum may be considered as discrete. Pressure broadening of the individual rotational lines helps to minimize the pulse shape distortion. Because δt_2 is inversely proportional to the gas pressure, it becomes $\approx$10 ps at 10 atm. Numerical calculations demonstrate that pulses longer than 20 ps can propagate without appreciable distortions. In a 3-atm amplifier filled with a regular gas mixture, pulses as short as τ_0=60 ps may be amplified without appreciable distortions. A shorter pulse will experiense less SSG, due to worse bandwidth matching to the gain spectrum, and gradual expansion of the pulse duration. That correlates with our experimental results, in which we observed a performance degradation when τ_0=30 ps sliced pulses were injected into the amplifier.

V. Scaling-up: prospects and limitations

In conclusion, let us consider the possibilities and principal limitations for further scale-up of single-beam picosecond CO_2 laser systems. To be more specific, a TE laser module of a moderate 10-cm aperture size and up to 10 atm pressure will be considered as a final amplifier. Such devices are feasible with x-ray and e-beam preionisation of the discharge volume.

In view of the presently demonstrated $I \approx 10$ GW/cm^2 flux at the amplifier output, it is reasonable to project $\approx$ 1 TW peak power extraction in $\approx$ 50-ps pulse after a second amplifier of 10-cm aperture. Our experimental data indicate that 3 passes through a 120 cm long amplifier would be adequate for the required 50-times power gain asuming that the final amplifier is of the same 3-atm pressure and specific energy loading as the present ATF amplifier.

A 10-atm x-ray or e-beam preionised CO_2 discharge module is a better candidate for a final amplifier, providing the prospect for even higher peak power via a combination of output energy increase and pulse shortening. Under higher energy loading ≈ 1.5 kJ/l attainable with such devices and because of optimisation of the normalised electric field, E/P, with more powerfull external ionisation, the specific energy storage at the upper vibrational CO_2 (001) laser level increases ≈ 8 times, in comparison with a 3-atm UV-preionised discharge, reaching value of 120 J/l. Faster rotational relaxation, $\tau_R \approx 20$ ps, and higher saturation fluence, $E_s^* \approx 500$ mJ/cm^2, complete the argument in favour of the energetic feasibility to extract up to $I = 100$ GW/cm^2 flux from 10-atm amplifier in a 50-ps pulse. With the additional ability to sustain shorter laser pulses, the projected 10-cm aperture high-pressure amplifier module could produce laser beams of more than 10 TW peak power. This conclusion conforms to another similar prognosis of P.Corkum[5] made after a demonstration of up to 1 GW peak power in a 1-mm^2 CO_2 picosecond laser beam.

Practical limitations to the intensity escalation in the picosecond CO_2 laser beams may be set by such detrimental effects as optical component (windows, mirrors) damage and gas breakdown. The analysis of the optical breakdown threshold data drives us to the conclusion that optical window damage will be the major limitation to energy scaling of picosecond CO_2 lasers. However, under the assumption of the avalanche electron multiplication mechanism for optical breakdown,[9] laser pulse shorterning should provide a nearly proportional increase of the finite flux that may be transmitted through the window without its damage. For example, E_{tA}=0.5 J/cm^2 was measured for a NaCl window with 2-ps CO_2 laser pulses;[5] equivalent to I_{tA}=0.25 TW/cm^2.

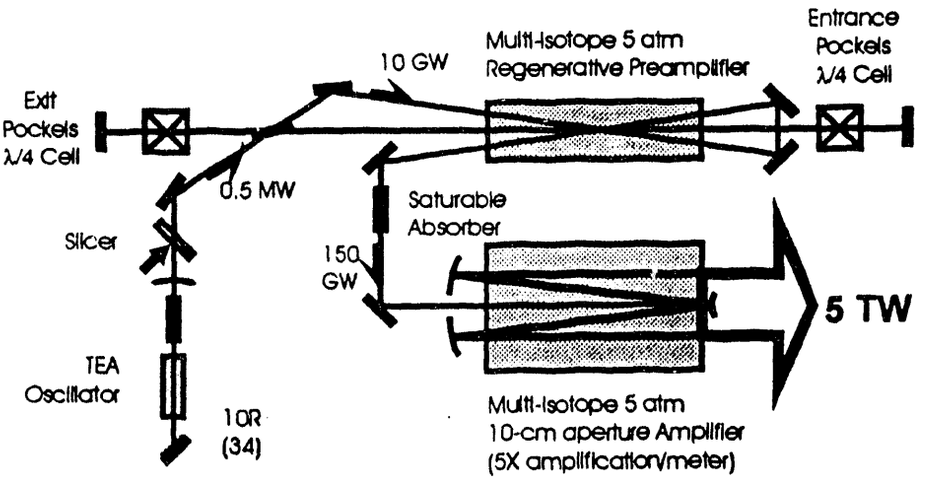

Figure 7: Multi-isotope CO_2 laser system project.

In order to amplify pulses as short as a few picoseconds, a multi-isotope laser gas mixture may be used. Typical for such mixture, smoothing of the gain spectrum results also in a noticable SSG drop, and two multipass amplifier stages are not enough any more to extract an output energy close to a potential limit of the system. Instead of using an extra stage, we consider in Fig.7 another option: a single-pulse regenerative amplifier in a first stage. Its output is limited by $\approx$10 GW by a Pockels cell optical damage. Hence, the additional two passes through the same amplifier discharge-cell will follow. And the final 10-cm aperture amplifier should increase the peak output to 5 TW in nearly linear regime.

A CO_2-pumped ammonia amplifier may be another promising approach to ultra- high-power picosecond IR laser systems.[10] The advantages of such a scheme are: the use of broad-bandwidth multiatomic molecular spectra favorable for short pulse amplification, and the possibility to use relatively simple nanosecond TEA CO_2 oscillator-amplifier systems as pump sources for an efficient energy transfer from the pump pulse to the picosecond pulse copropogating inside a molecular amplifier.

When 0.1% NH_3 is diluted in 6 atm of N_2 or Ar, pulses as short as 10 ps can be amplified without appreciable distortion within the 926-938 cm^{-1} spectral range covered by regular NH_3 band overlapping transitions. Maximum gain corresponds to the 9P(34) CO_2 transition while the 9R(30) CO_2 transition may be used for pumping. Experimentally, a single pass gain of 21.8 dB was observed by this scheme, when $\approx$25 MW/cm^2 TEA CO_2 laser pulse was used to pump the ν_2=1 NH_3 vibrational level. NH_3 collisional relaxation time, $\approx$20 ns, puts certain limitation on the optimal duration of the pump pulse. Up to 60 dB gain is predicted, when a 10- ns, 3 J/cm^2 pump pulse is used.[9]

VI. References

1. E. Yablonovich and J. Goldar, *Appl. Phys. Lett.*, vol.25, 580 (1974); R.Kesselring, A.W. Kahlin, H.J. Schotsau, and F.K. Kneubuhl, *IEEE J. Quant. Electron.*, vol.29, 997 (1993).

2. A. Laubereau, L. Greiter, W. Kaiser, *Appl. Phys. Lett.*, vol.25, 87 (1974); T. Elsaesser, A. Seilmeir, W. Kaiser, *Opt. Commun.*, vol.44, 293 (1983).

3. S.A. Jamison, A.V. Nurmikko, and H.J. Gerritsen, *Appl. Phys. Letts.*, vol.29, 640 (1976).

4. A.J. Alcock and P.B. Corkum, *Can. J. Phys.*, vol.57, 1280 (1979).

5. P.B. Corkum, *IEEE J. Quant. Electron.*, vol.QE-21, 216 (1985).

6. I. Ben-Zvi, *Advanced Accelerator Concepts, AIP Conference Proceedings* vol.279, 590 (1993).

7. V.T. Platonenko and V.D. Taranukhin, *Sov.J.Quant.Electron.*, vol.13, 1459 (1983).

8. F. Kannari, *STI Optronics Technical Note*, Draft (1988).

9. See discussion to M.D. Crisp, *NBS Special Publ.*, #387, 80 (1973).

10. J.D. White and J. Reid, *IEEE J. Quant. Electron.*, vol.29, 201 (1993).

ACKNOWLEDGMENTS

Authors wish to thank scientists and technical personnel of the ATF headed by I. Ben-Zvi who contributed in bringing the CO_2 laser system to operation. Special thanks to W. Kimura (STI Optronics) and F. Kannari (Keio University, Yokohama) for providing computer simulations used to illustrate the analysis of the picosecond CO_2 laser pulse amplification.

This work was supported by the Department of Energy, Contract No. DE-ACO2-76CH00016 and No. DE-AC06-83ER40128.

DISCLAIMER

DATE
FILMED
4/20/94
END